© 2016. Published by The Company of Biologists Ltd | Development (2016) 143, 3895-3906 doi:10.1242/dev.134601

STEM CELLS AND REGENERATION

RESEARCH ARTICLE

Emergence of dorsal-ventral polarity in ESC-derived retinal tissue

Yuiko Hasegawa[1,2], Nozomu Takata[1,2], Satoru Okuda[1,2], Masako Kawada[1,2], Mototsugu Eiraku[1,2,*] and Yoshiki Sasai[1,‡]

ABSTRACT

We previously demonstrated that mouse embryonic stem cell (mESC)-derived retinal epithelium self-forms an optic cup-like structure. In the developing retina, the dorsal and ventral sides differ in terms of local gene expression and morphological features. This aspect has not yet been shown *in vitro*. Here, we demonstrate that mESC-derived retinal tissue spontaneously acquires polarity reminiscent of the dorsal-ventral (D-V) patterning of the embryonic retina. Tbx5 and Vax2 were expressed in a mutually exclusive manner, as seen *in vivo*. Three-dimensional morphometric analysis showed that the *in vitro*-formed optic cup often contains cleft structures resembling the embryonic optic fissure. To elucidate the mechanisms underlying the spontaneous D-V polarization of mESC-derived retina, we examined the effects of patterning factors, and found that endogenous BMP signaling plays a predominant role in the dorsal specification. Further analysis revealed that canonical Wnt signaling, which was spontaneously activated at the proximal region, acts upstream of BMP signaling for dorsal specification. These observations suggest that D-V polarity could be established within the self-formed retinal neuroepithelium by intrinsic mechanisms involving the spatiotemporal regulation of canonical Wnt and BMP signals.

KEY WORDS: Morphogenesis, Organoid culture, Pattern formation, Retinal development

INTRODUCTION

Vertebrate eye development is a complex event that requires rigorous polarity regulation with specific gene expression patterns. In the murine eye, the optic primordium starts to evaginate laterally from the diencephalon at embryonic day (E)8.0 and forms the optic vesicle at ∼E9.5. Subsequently, the distal portion of the optic vesicle invaginates to form the optic cup, which is composed of double-walled neuroepithelium at E10.5. The inner epithelium gives rise to neural retina (NR) and the outer wall becomes retinal pigmented epithelium (RPE).

Regarding the formation of dorsal-ventral (D-V) polarity in the NR, it is well known that specific transcription factors have a critical role in D-V patterning. In mouse and chick optic development, Tbx2 and Tbx5 (Behesti et al., 2009; Koshiba-Takeuchi et al., 2000), members of the conserved T-box gene family, have been identified as key regulators for dorsal specification. In particular, *Tbx5* is specifically expressed in the most dorsal regions (Behesti et al., 2006) and misexpression of *Tbx5* results in dorsalization of NR and misrouting of the retinal ganglion cell (RGC) projection axon (Koshiba-Takeuchi et al., 2000). On the other hand, *Vax2*, which belongs to a homeobox gene subfamily, is a key regulator for ventral specification. Previous studies have shown that impairment of *Vax2* function resulted in ocular coloboma, dorsalization of NR, interference of normal ventral axonal projection and alterations in cone opsin distribution (Mui et al., 2002; Alfano et al., 2011).

Optic cup formation does not occur by axisymmetric deformation, because a shallow furrow leading to the optic stalk (called the optic fissure or choroid fissure) forms on the ventral surface of optic cup, where RGC axons, and later the hyaloid artery, pass through. As the optic cup deepens, the fissure becomes a slit and finally closes completely (Morse and McCann, 1984). Proper formation and closure of the optic fissure are important for the correct formation of the optic nerve and hyaloid artery, yet the deformation process still remains incompletely understood.

Previous studies have suggested that bone morphogenetic protein (BMP) and Sonic hedgehog (Shh) are candidates for the upstream signal of Tbx5 and Vax2 within the context of D-V polarization (reviewed by Yang, 2004; Zhao et al., 2010; Kobayashi et al., 2010). In early mouse optic vesicles, *Bmp4* is expressed on the distal portion and subsequently confined to the dorsal portion (Furuta and Hogan, 1998; Behesti et al., 2006). Ectopic expression of *Bmp4* in the early optic cup induces the expansion of *Tbx5* and reduction of *Vax2* (Koshiba-Takeuchi et al., 2000). Wnt signaling is also known to be involved in D-V polarization of retinal tissue (Veien et al., 2008; Hägglund et al., 2013). Wnt2b (Wnt13) is localized in dorsal RPE at an early optic vesicle stage in mice and chicks (Cho and Cepko, 2006; Steinfeld et al., 2013). In mice deficient in the Wnt receptor or its downstream component, dorsal retinal markers such as *Bmp4* and *Tbx5* are diminished (Zhou et al., 2008; Esteve et al., 2011; Hägglund et al., 2013). Although these previous reports suggest that both BMP signaling and canonical Wnt signaling profoundly affect the dorsal retinal specification, the underlying mechanisms of crosstalk between these signals are poorly understood.

We previously reported the formation of 3D optic tissue from mouse and human embryonic stem cells (mESCs and hESCs, respectively) and using a serum-free culture of embryoid body-like aggregates with a quick aggregation SFEBq method (Eiraku et al., 2011; Nakano et al., 2012). Addition of Matrigel to the initial medium induced the homogenous ESC aggregate to differentiate into a retinal structure with dynamic morphological changes such as formation of an optic vesicle-like structure and an optic cup-like structure.

In this study, taking advantage of the simplicity and manipulability of this culture system, we focused on the spontaneous D-V polarity formation and its underlying mechanisms during optic morphogenesis. We found evidence that the mESC-derived retinal tissue spontaneously acquires D-V polarity with specific gene expression, and sequential signals of

[1]Laboratory for Organogenesis and Neurogenesis, RIKEN Center for Developmental Biology, 2-2-3, Minatojima-Minamimachi, Chuo, Kobe 650-0047, Japan. [2]Laboratory for in vitro Histogenesis, RIKEN Center for Developmental Biology, 2-2-3, Minatojima-Minamimachi, Chuo, Kobe 650-0047, Japan.
‡Deceased

*Author for correspondence (eiraku@cdb.riken.jp)

M.E., 0000-0002-9433-9085

Received 28 December 2015; Accepted 1 September 2016

Development (2016) 143, 3895-3906 doi:10.1242/dev.134601

Wnt and BMP cooperatively control the D-V polarization of the retinal neuroepithelium.

RESULTS

D-V regionalization in mESC-derived retinal tissue

To visualize the D-V polarity, we first raised antibodies against the dorsal retinal marker Tbx5 and the ventral retinal marker Vax2. Consistent with mRNA expression patterns as previously reported (Behesti et al., 2006; Mui et al., 2002), immunostaining using these antibodies showed that Tbx5 was expressed on the dorsal side of the embryonic optic cup, in particular, in the dorsal quadrant of the NR, whereas Vax2 was expressed in the ventral NR and RPE [Fig. 1A at E10.5, Fig. 1B at E9.75 (Fig. 1B acquired with a light-sheet microscope), Fig. S1A at E9.5].

We next examined the expression patterns of Tbx5 and Vax2 in the self-organized optic cup-like tissues derived from mESCs (*Rx::EGFP*) with these antibodies (Fig. 1C). In most cases, Chx10 is specifically expressed in the inner epithelium in which the expression level of Rx (retina and anterior neural fold homeobox, also known as Rax) is higher than in RPE (Fig. 1D,E and Fig. S1B,C). In some cases, Chx10 is also expressed in the more proximal part rather than the hinge of the ESC-derived optic cup (Fig. S1D). We found that mESC-derived retinal tissue is regionalized into three domains by different marker expression patterns: $Tbx5^{+}/Vax2^{-}$ (domain 1), $Tbx5^{-}/Vax2^{-}$ (domain 2) and $Tbx5^{-}/Vax2^{+}$ (domain 3) (Fig. 1F-H). We observed that 21% of ESC-derived optic cups had all three domains, as seen in embryonic retina (Behesti et al., 2006), but optic cups without domain 1 or domain 2 were also observed (Fig. S1E,F). In addition, Coup-TFI (Nr2f1) and Coup-TFII (Nr2f2) are specifically expressed at the ventral and dorsal side of embryonic retina, respectively (Satoh et al., 2009). In mESC aggregates, Tbx5 expression was seen on the $Coup\text{-}TFI^{weak}$ and $Coup\text{-}TFII^{strong}$ side, which is suggestive of the dorsal side, and Vax2 was expressed on the $Coup\text{-}TFI^{+}$ and $Coup\text{-}TFII^{weak}$ side, which is suggestive of the ventral side (Fig. 1I-L). These results suggest that D-V patterning in terms of marker expression was spontaneously generated in mESC-derived retinal tissue in a less-reproducible manner than *in vivo*.

To confirm the formation of D-V polarity in mESC-derived retinal tissue at later stages, we conducted long-term culture. In the embryonic optic cup, the ventral side of the NR is connected to the diencephalon through the optic disc and optic stalk, in which neurofilament $(NF)^{+}$ optic nerves later pass (Fig. 1M,N). The optic disc is a small region marked with Vax2 and Pax2 co-expression (Fig. 1M,N). When mESC-derived NR was isolated and cultured in collagen gel until day 17, we observed that thick bundles of axons extended from a few points of the NR tissue. (Fig. 1O, Fig. S1G,H). Immunohistochemistry revealed that these axon outlet points consisted of $Pax2^{+}/Vax2^{+}$ condensed tissues flanked with a NF^{+} component, as seen in the embryonic optic disc (Fig. 1P-S). We also found that in some cases, NF^{+} axons extended from a relatively large area sparsely expressing Pax2 and converged thick bundles of axons surrounding the aggregate (Fig. S1I,J). Taken together, these results indicate that the D-V polarity with patterned gene expression and an optic disc-like structure emerged in mESC-derived retinal tissue.

Self-formation of optic fissure-like structure

In the developing optic cup, the ventral-most portion has a cleft structure, called the optic fissure. Interestingly, multi-photon microscope observation revealed that the mESC-derived optic cup had a non-axisymmetric shape and occasionally included cleft structures reminiscent of embryonic optic fissure on one side (62% of optic cup-like structures, n=37, Fig. 2A-C, Movie 1). The 3D reconstruction of immunostained tissues demonstrated that the expression patterns of Tbx5 and Vax2 are mutually exclusive (Fig. 2D), and the fissure-like structure frequently formed in the $Tbx5^{-}$ domain of the mESC-derived optic cup-like structure (69%, n=13, Fig. 2E,F). These results suggest that a choroid fissure-like structure can also self-form in retinal tissues derived from mESCs.

We next sought to analyze how the fissure was folded during *in vitro* optic cup formation by time-lapse imaging using an incubator-docked multi-photon microscope (Eiraku et al., 2011; Movie 2). As we reported previously, before the onset of invagination, the distal portion of the optic vesicle thickens (Fig. 2I, red arrow). We noticed that the apical surface of the hinge region, a border between NR and RPE, became acutely angled at one side during cup formation (Fig. 2I, red circle, and M). At the opposite side, the apical surface remained gently angled with continuous curvature (Fig. 2I, yellow circle, and M). As invagination proceeds and the cup deepens, the NR grows laterally (Fig. 2J,K) and the marginal tissue between NR and RPE grows more distally except for the side with the gently angled apical surface (Fig. 2G,H, yellow arrows and Fig. 2L). As a result, the optic cup had a valley structure reminiscent of the optic fissure as seen *in vivo*. These observations suggest that the self-formed optic cup not only exhibits a D-V marker expression profile but also a morphology characteristic of D-V polarity, and the optic fissure-like structure could be formed in a self-organized manner in mESC culture.

Endogenous BMP signaling regulates D-V specification in mESC-derived retinal tissue

Previous studies have implicated the roles of BMP and Shh signals in the D-V patterning of the embryonic retina. In the developing eye, the optic cup is exposed to these external cues from surrounding non-retinal tissues such as periocular mesenchyme, diencephalic neuroepithelium and surface ectoderm (Furuta and Hogan, 1998; Fuhrmann et al., 2000; Kobayashi et al., 2010; Steinfeld et al., 2013). However, in our ESC culture, interactions with these tissues are absent. To elucidate retinal epithelium-intrinsic mechanisms underlying the D-V polarization, we next examined roles of endogenous BMP and Shh signaling on the expression of *Tbx2*, *Tbx3*, *Tbx5* and *Vax2* mRNA on day 7-8.5 (Fig. 3A). RT-qPCR analysis revealed that BMP4 treatment robustly elevated the expression levels of *Tbx2*, *Tbx3* and *Tbx5* mRNA, and substantially suppressed *Vax2* expression. Conversely, dorsomorphin, an antagonist of the BMP ligand, strongly suppressed *Tbx2*, *Tbx3* and *Tbx5* expression and moderately increased *Vax2* expression (Fig. 3B and Fig. S2A). On the other hand, neither a Shh signaling agonist nor an antagonist [Smoothened agonist (SAG) and cyclopamine-KAAD] had any effect on *Vax2* expression. Furthermore, *Tbx5* expression was suppressed by treatment with SAG (Fig. S2B). Collectively, these findings suggest that endogenous BMP signaling predominantly regulates D-V marker expression in mESC-derived retinal tissues, whereas Shh signaling has a minor function.

We next confirmed these results by immunohistochemistry. mESC-derived retinal tissues were treated with BMP4 or dorsomorphin from day 7 and analyzed with antibodies against phosphorylated Smad1/5/8 (pSmad) and Tbx5. In the mouse developing eye, the dorsal NR and RPE near the hinge region (pre-RPE) was positive for pSmad (Fig. S3D,E). In ESC culture, *Bmp4* mRNA and pSmad were broadly detected at the distal portion of day 7 optic vesicle. By contrast, Tbx5 was more locally expressed

Development (2016) 143, 3895-3906 doi:10.1242/dev.134601

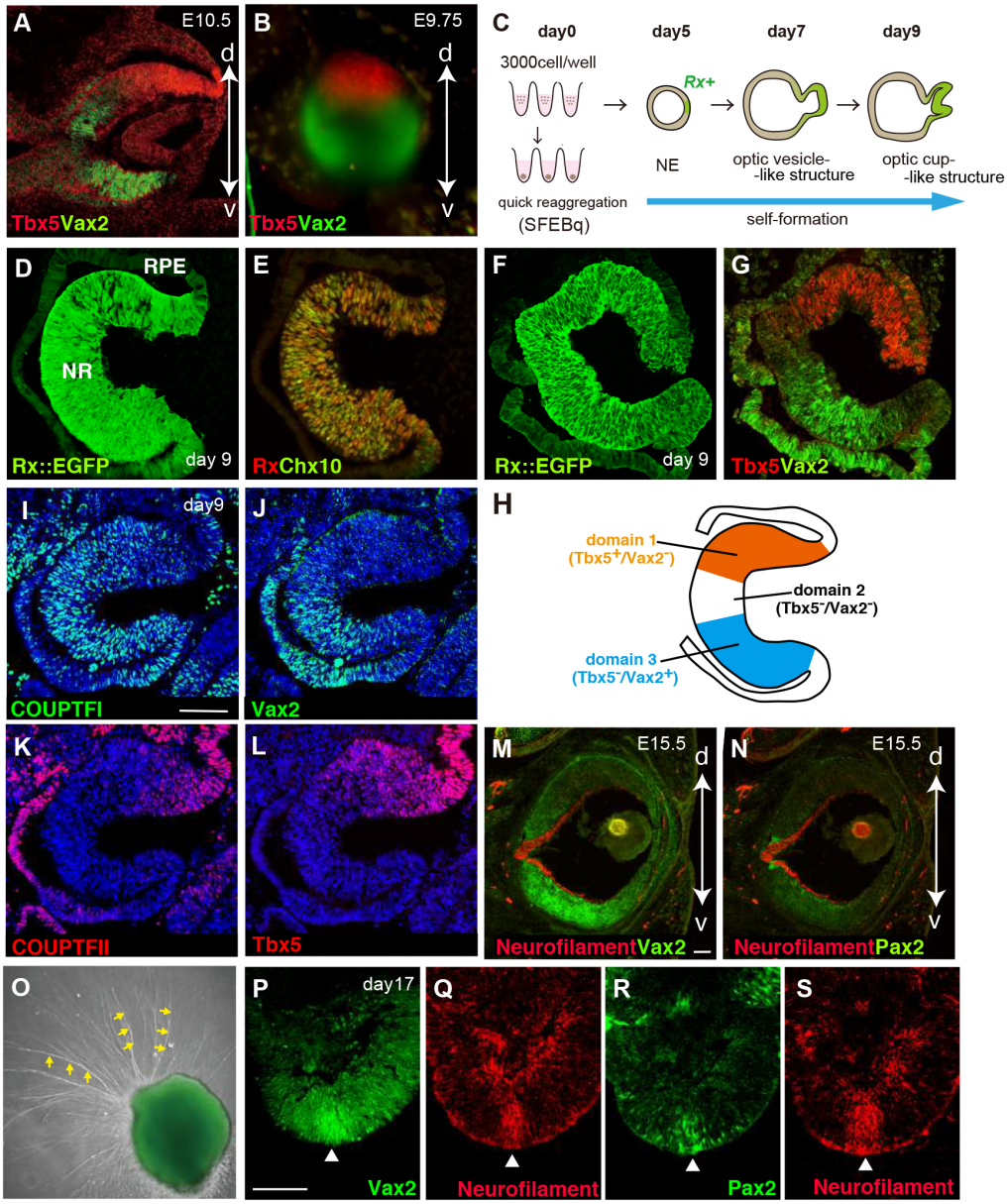

Fig. 1. Differential dorsal-ventral markers emerge in mESC-derived retinal tissue. (A,B) Immunostaining for Tbx5/Vax2 in mouse embryonic eye. A coronal section (E10.5) (A) and a frontal view image of whole immunostaining (E9.75) by light-sheet microscope (B). (C) Procedure for self-formation of the mESC-derived retinal tissue by SFEBq. (D-G) Immunostaining for Rx::EGFP (D,F), Rx/Chx10 (E) and Tbx5/Vax2 (G) in mESC-derived optic cup. Sections in D and E are the same, as are F and G. (H) Schematic for three domains, which are regionalized by Tbx5 and Vax2 expression pattern *in vitro*. (I-L) Immunostaining of mESC-derived retinal tissue, for Coup-TFI (I), Vax2 (J), Coup-TFII (K) and Tbx5 (L). Sections in I and J are the same, as are K and L. (M,N) Immunostaining for neurofilament (NF) 200kDa and Vax2 (M), and NF and Pax2 (N) on coronal section of mouse E15.5 eye. Two triangular-shaped groups of cells flanking the NF^+ axons, which were double positive for Vax2 and Pax2, represent optic disc. (O-S) Mature mESC-derived retinal tissues after long-term culture. Yellow arrows indicate bundles of axons (O). NF^+ axons (Q,S, red) existed throughout the $Vax2^+$ (P, green) region and $Pax2^+$ region (R, green) on day 17. White arrowheads indicate the exit point. Sections in P and Q are the same, as are R and S. NE, neuroepithelium; NR, neural retina; RPE, retinal pigment epithelium; d-v, dorsal-ventral retina. Scale bars: 100 µm.

(Fig. S3F-I,N). On day 9, Tbx5 expression mostly overlapped with the region marked with *Bmp4* mRNA and pSmad (Fig. 3C and Fig. S3J-N). We also found $Tbx5^+$/$pSmad^+$ cells not only in dorsal NR but also in the pre-RPE region (Fig. 3C). Such dynamics of BMP signaling molecules are consistent with that seen during mouse optic cup formation (Yun et al., 2009). Treatment with exogenous BMP4 upregulated both Tbx5 and pSmad immunoreactivities, whereas treatment with BMP antagonist completely diminished both signals (Fig. 3D-F). Notably, when optic vesicles were treated with BMP4 or dorsomorphin, invagination was disturbed in both cases (Fig. 3C-E, Fig. S3A,B), but there was little effect on NR or RPE specification (Fig. S3C,D)

Development (2016) 143, 3895-3906 doi:10.1242/dev.134601

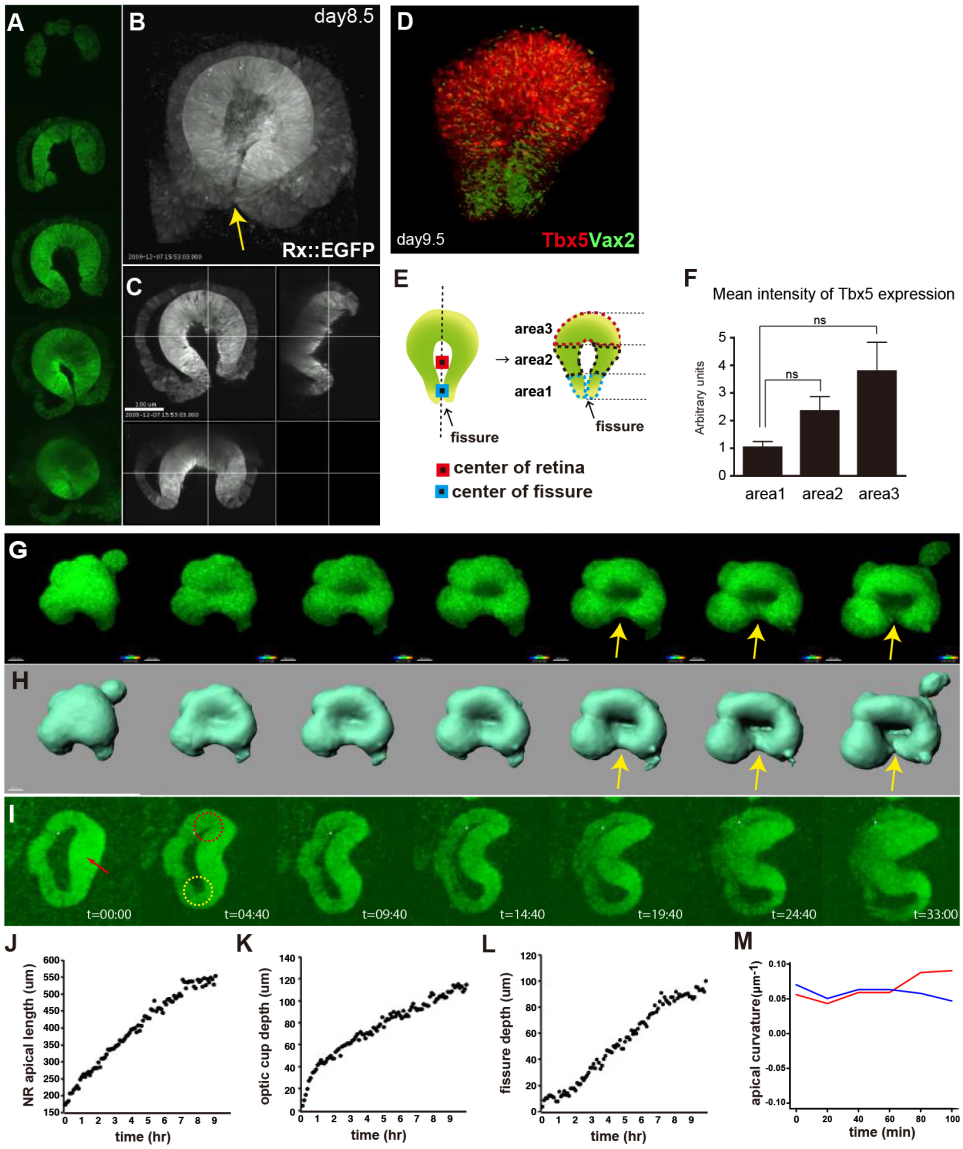

Fig. 2. A fissure forms spontaneously in the mESC-derived optic cup-like structure during morphogenesis. (A-C) Surface-rendering 3D reconstruction images by two-photon microscopy of mESC-derived optic cup on day 8.5 using the *Rx::EGFP* cell line. (A) *Z*-directional serial images. (B) A 3D reconstruction image with a fissure (yellow arrow) (see Movie 1). (C) Top left, vertical view of a fissure; top right, lateral view; bottom left, anterior view. (D) 3D reconstruction images of serial sections of Tbx5 and Vax2 immunostaining. The RPE region was removed. (E,F) Experiment to assess variation of Tbx5 expression in a fissure of mESC-derived optic cup. After whole-mount immunostaining, 3D images were obtained by a light-sheet microscope. An image projected on a plane was oriented to face the hollow structure toward the front. The center of Rx^+ NR and the center of the fissure were calculated manually. (E) A straight line to connect these two points was drawn and divided equally among the three. Area 1 was defined as the closest trisected region against the fissure, area 2 was defined as the middle trisected region and area 3 was defined as the most distant trisected region. (F) Expression gradient of mean intensity of Tbx5 staining (mean±s.e.m. of *n*=3 experiments). (G-M) Four-dimensional (4D) imaging analysis of fissure formation. Total observational time was 35 h with acquisitions every 20 min (time is shown on bottom right of panels in I in h:min). The yellow arrows indicate the fissure (see Movie 2). (G) Raw sequential images. (H) Surface-rendering 4D reconstruction images. (I) Cross sectional raw images along dorsal-ventral axis. (J-M) Quantification of tissue dynamics demonstrated in Movie 2. NR apical length (J), optic cup depth (K), fissure depth (L) and apical curvatures (red, dorsal; blue, ventral; M) were measured. Scale bars: 100 μm (A), 50 μm (G). ns, not significant.

By whole mount immunostaining, we confirmed these results in a 3D context. Volumes of tissues expressing Tbx5 were increased by BMP4 treatment and decreased with dorsomorphin treatment. Conversely, the volume of Vax2-expressing tissue increased with dorsomorphin treatment and decreased with BMP4 (Fig. S2C). Together, these results suggest that BMP signaling is spontaneously activated in a spatially ordered manner and that it plays a crucial role in specifying the dorsal identity of mESC-derived retinal tissue.

Canonical Wnt signaling evokes dorsal specification through BMP signaling in early mESC-derived retinal tissue

To elucidate how BMP signaling is spatiotemporally regulated in mESC-derived retinal tissues, we next focused on canonical Wnt

Development (2016) 143, 3895-3906 doi:10.1242/dev.134601

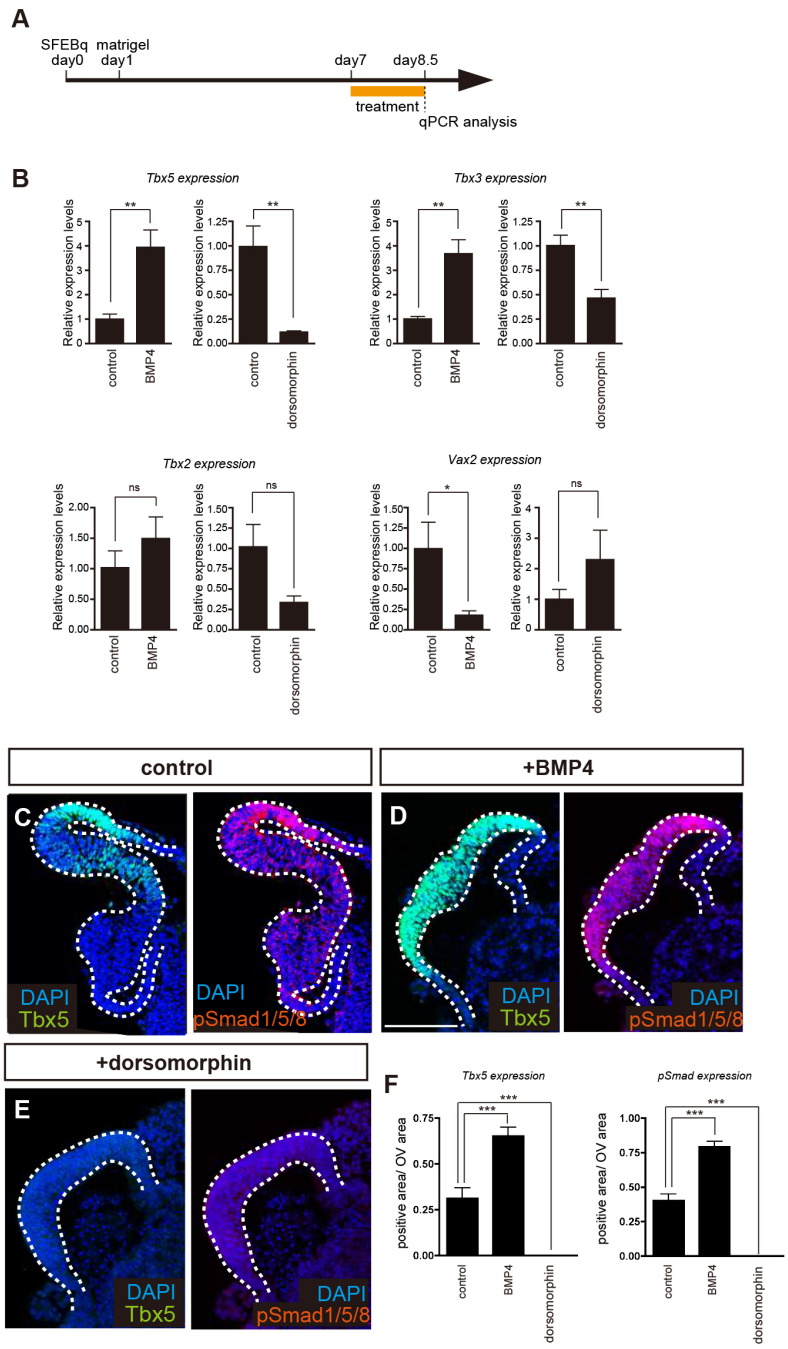

Fig. 3. Endogenous BMP signaling regulates D-V marker expression in mESC-derived retinal tissue. (A) Schematic of inhibitor assay. (B) From day 7, Rx^+ aggregates were treated with 0.2 nM BMP4 or 1 µM dorsomorphin and qPCR analysis was performed on day 8.5. (C-E) Immunostaining of mESC-derived retinal tissue for Tbx5 and pSmad after treatment with medium alone (control, C), 0.2 nM BMP4 (D) or 1 µM dorsomorphin (E) on day 7-8.5. White dotted lines indicate $Rx::EGFP^+$ neuroepithelium. (F) Quantification of $Tbx5^+$ area and $pSmad^+$ area versus $Rx::EGFP^+$ by immunostaining. Scale bars: 100 µm. ***P<0.001, **P<0.01, *P<0.05 (Student's t-test one-way ANOVA with Tukey's post hoc test). Data are mean±s.e.m. of n=4.; ns, not significant.

signaling, which is another candidate for the dorsal regulator of optic vesicle at an earlier stage. To monitor canonical Wnt signaling dynamics during *in vitro* cup formation, we established transgenic cell lines in which fluorescent proteins are under control of a promoter with LEF1/Tcf binding domains (*Rx::EGFP/7tcf::mCherry* and *Rx::EGFP/7tcf::H2BtdTomato*; Takata et al., 2016). Using these cell lines, we performed live imaging analysis on day 2.5-7.5 and on day 7-8 (Movies 3 and 4). With maturation of NR, the intensity of Rx::EGFP strengthened throughout the retinal neuroepithelium, and at the same time, the canonical Wnt reporter was activated at a border between retinal neuroepithelium and non-retinal neuroepithelium by day 6 (Fig. 4A, arrowheads). On day 6.5, whereas Rx::EGFP expression was gradually attenuated at the proximal region of one side of the optic vesicle, Wnt signaling became augmented at this region (Fig. 4A). Importantly, the NR on the side with the stronger Wnt activation invaginated faster than the opposite side (Fig. 4B), consistent with the observation of non-axisymmetric morphogenesis with fissure formation (Fig. 2J). From these results, we hypothesized that locally activated canonical Wnt signal might be involved in BMP signal induction in a spatially-

Development (2016) 143, 3895-3906 doi:10.1242/dev.134601

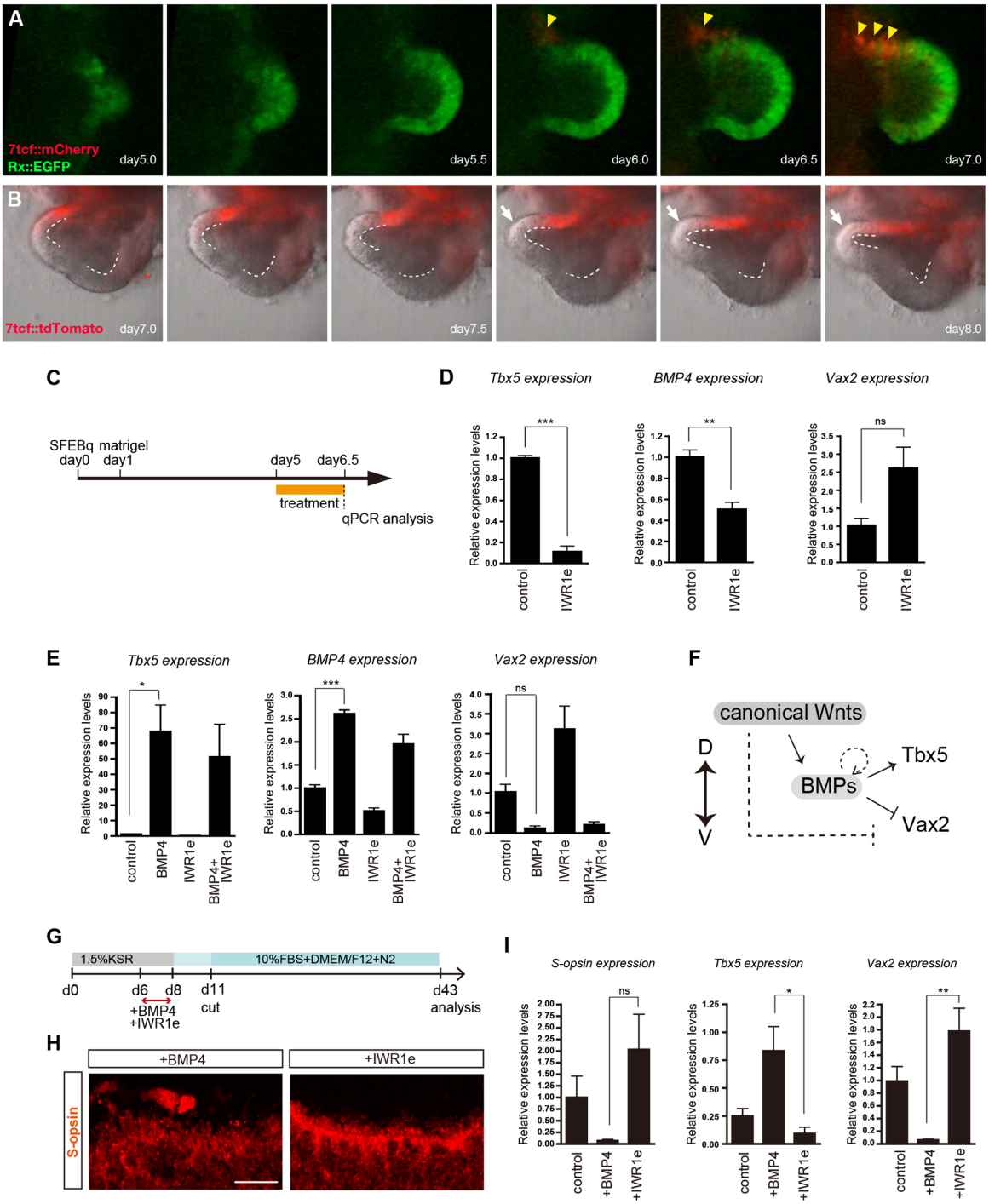

Fig. 4. Canonical Wnt signaling induces dorsal specification in the early mESC-derived optic vesicle-like structure. (A) Live imaging for emergence of canonical Wnt signaling in Rx$^+$ mESC-derived retinal tissue on day 2.5-7.5. Wnt activity was detected at the proximal region on one side of the optic vesicle on day 6.5 (arrowheads; see Movie 3). (B) Live imaging for visualization of asymmetrical expression of canonical Wnt signaling during invagination, using *Rx::EGFP* and *7tcf::H2BtdTomato* cell lines. White dotted lines indicate apical side of retinal neuroepithelium. White arrows indicate presumptive dorsal hinge region, which started to invaginate (see also Movie 4). (C) Schematic of inhibitor assay to understand involvement of canonical Wnt signaling for D-V polarization at early differential stage. qPCR analysis was performed after treatment with 0.5 µM IWR1-endo (D) or in combination with 0.05 nM BMP4 (E) on day 5-6.5. (F) Model of sequential activities of canonical Wnt and BMP signaling for formation of D-V polarity. (G-I) BMP and Wnt affect later retinal development. (G) Schematic of experiment. After 0.1 nM BMP4 or 0.5 µM IWR1-endo treatment on day 6-8, Rx$^+$ retinal neuroepithelium was cut and cultured until day 43. (H) Immunostaining of S-opsin and Rx::EGFP on day 43 in the matured mESC-derived retinal tissue. (I) qPCR analysis results on day 43. ***P<0.001, **P<0.01, *P<0.05; ns, not significant (Student's *t*-test and one-way ANOVA with Tukey's post hoc test). Data are mean±s.e.m. of n=3. Scale bar: 20 µm.

Development (2016) 143, 3895-3906 doi:10.1242/dev.134601

ordered manner and could regulate D-V polarization of mESC-derived retinal tissue.

We next examined the effects of a Wnt agonist and antagonist on D-V marker expression (Fig. 4C and Fig. S4B). In our mESC culture, Wnt3a treatment from day 5 resulted in upregulation of *Tbx5* and downregulation of *Vax2* (Fig. S4A). *Bmp4* expression was also modestly increased by Wnt3a treatment (Fig. S3A). In contrast, when mESC aggregates were treated with the canonical Wnt antagonist IWR1-endo at day 5-6.5, both *Bmp4* and *Tbx5* expression were significantly repressed, and *Vax2* expression was increased, suggesting that endogenous canonical Wnt signaling is involved in the dorsal initiation through BMP4 induction (Fig. 4D). Moreover, reduction of *Tbx5* by inhibition of the canonical Wnt pathway was dramatically overturned by the addition of BMP4 (Fig. 4E). We also found that the level of *Bmp4* mRNA was slightly upregulated by BMP4 treatment, and *Bmp4* and *Tbx5* were significantly reduced upon treatment with dorsomorphin, suggesting that Bmp4 signaling is activated by an autocrine effect (Fig. 4E and Fig. S4C). Collectively, these results suggest that the canonical Wnt pathway acts upstream of BMP signaling in dorsal retina initiation and specification in mESC culture (Fig. 4F).

We next examined whether these dorsalizing signals could affect D-V characteristics in the mature retinal tissue generated from mESCs. Previous studies have shown that short-wavelength (S)-opsin is more highly expressed on the ventral side of mouse retina (Applebury et al., 2000). After treatment with BMP4 or IWR1-endo on day 6-8, the aggregates were transferred to long-culture medium and cultured until NR became fully mature on day 43 (Fig. 4G). Compared with controls, *S-opsin* and *Vax2* expression were suppressed in BMP4-treated NR. However, IWR1-endo treatment increased the expression of *S-opsin* and suppressed *Tbx5* expression (Fig. 4H,I). The level of expression of *Efnb2* (ephrin B2), a dorsal marker of mature NR, was slightly increased by BMP4 treatment, whereas expression of *Ephb2* (Eph receptor B2), a ventral marker of matured NR, decreased (Peters and Cepko, 2002; Fig. S4D). Collectively, we confirmed that early canonical Wnt activation could regulate D-V polarization at both the early and later stages.

Locally activated canonical Wnt signaling induced expression of Tbx5 in the neighboring retinal neuroepithelium

To further elucidate the spatiotemporal regulation of Wnt and BMP signaling, we next examined the timing of Wnt activation and D-V marker onset. On day 6, neither 7tcf::H2BtdTomato nor Tbx5 expression was observed in the Rx^+ optic vesicle. By contrast, Vax2 expression is widespread at this early optic vesicle stage (Fig. 5A,B). Tbx5 expression was first detected on day 6.5-7 after 7tcf::H2BtdTomato expression emerged at the proximal region (Fig. 5C-E and scheme in G). Interestingly, Tbx5 and pSmad were induced at the region adjacent to the 7tcf::H2BtdTomato$^+$ domain and Vax2 expression was now localized to the opposite end (Fig. 5F; Fig. S5A-D). BMP-activated cells ($pSmad^+$) are a distinct population from Wnt-activated cells (Fig. S5E). We also noticed that the size of the region positive for Tbx5 or pSmad varied in each aggregate. In contrast, the Wnt-activated area was constant, even when the induced optic vesicle varied in size (Fig. S5F,G). These observations are consistent with the idea that $Vax2^+$ retinal tissue is a default for D-V polarity formation and $Tbx5^+$ retinal tissue is induced by inductive signals involving Wnt and BMP (summarized in Fig. 6B).

To obtain further evidence that locally activated canonical Wnt signaling induces a dorsal identity in the neighboring domain, we performed local application of diffusible factors to the mESC-derived retinal neuroepithelium (Movie 5). In this experiment, to minimize the effect of endogenous canonical Wnt signaling, aggregates were pretreated with IWR1-endo on day 5.5-6 by bath application. After wash out of the reagent, the Wnt signaling agonist CHIR99021 (CHIR) was locally applied using a glass capillary (Fig. 5H). In a control pretreated with global IWR1-endo, both Tbx5 and 7tcf::H2BtdTomato expression were hardly seen (Fig. 5L). On the other hand, locally applied CHIR (co-injected with Alexa Fluor 647-dextrin) triggered 7tcf::H2BtdTomato signal only at the locus close to the application site after 12.5 h (Fig. 5I-K). Intriguingly, we found that Tbx5 expression was induced at the adjacent region of 7tcf::H2BtdTomato$^+$ tissue triggered by locally applied CHIR in Rx^+ retinal neuroepithelium on day 7 (Fig. 5M and scheme in N). In contrast, local application of BMP4 directly induced Tbx5 expression and upregulated pSmad at the site close to the applied position (Fig. 5O-P′,Q and Fig. S5H-O). In the case of local treatment with BMP4, we have never observed canonical Wnt upregulation at the site close to the applied position. Altogether, these results confirm the idea that localized canonical Wnt signaling elicits Tbx5 expression through spatial regulation of the BMP signal.

DISCUSSION

Here, we demonstrate that dorsal-ventral (D-V) polarization with patterned gene expression and non-axisymmetric morphogenesis spontaneously occurs in the mESC-derived retinal neuroepithelium. We also show that sequential local activity of canonical Wnt and BMP signaling are required for the spontaneous D-V polarization. These results suggest that retinal neuroepithelium is capable of self-organizing to form an optic cup-like structure with D-V polarity.

D-V regional specification emerges in self-formed retinal structure

Several reports have shown that Tbx5 and Vax2 act as master regulators for dorsal and ventral specification of developing retina, respectively (reviewed by Yang, 2004 and McLaughlin et al., 2003; Zhang and Yang, 2001; Peters and Cepko, 2002; Behesti et al., 2006). In this report, we demonstrate that mESC-derived retinal tissues are spontaneously regionalized into several domains marked with each of dorsal (Tbx5 and Coup-TFI) and ventral (Vax2 and Coup-TFII) markers. Additionally, at a later stage of mESC-derived retinal culture, Vax2 expression was seen in a $Pax2^+$ region in which Neurofilament$^+$ neurites were densely accumulated, mimicking embryonic optic disc – a ventral structure of the retina. Therefore, the $Tbx5^+$ and $Vax2^+$ regions in our culture indeed represent dorsal and ventral retinal characteristics, respectively. In a previous study, we showed that optic cup self-forms from mESCs in the absence of other tissues, such as lens placode and periocular mesenchymes (Eiraku et al., 2011). Therefore, the present results suggest that the D-V patterning in mESC culture could be achieved by intrinsic mechanisms of the retinal neuroepithelium.

However, we also noticed that the D-V patterning was not as reproducible as the embryonic optic cup formation in our culture system. In the developing eye, the NR consists of three regions: $Tbx5^+/Vax2^-$ (most dorsal; domain 1), $Tbx5^-/Vax2^-$ (domain 2) and $Tbx5^-/Vax2^+$ (most ventral; domain 3). Among mESC-derived retinal tissues, by contrast, only 21% were composed of all three domains. In other cases, the mESC-derived retinal tissue consisted of domains 1 and 3, or domains 2 and 3 (Fig. S1). Furthermore, it was observed that Chx10 occasionally extended its expression into the pre-RPE domain. Such variations in ESC culture, as well as

Development (2016) 143, 3895-3906 doi:10.1242/dev.134601

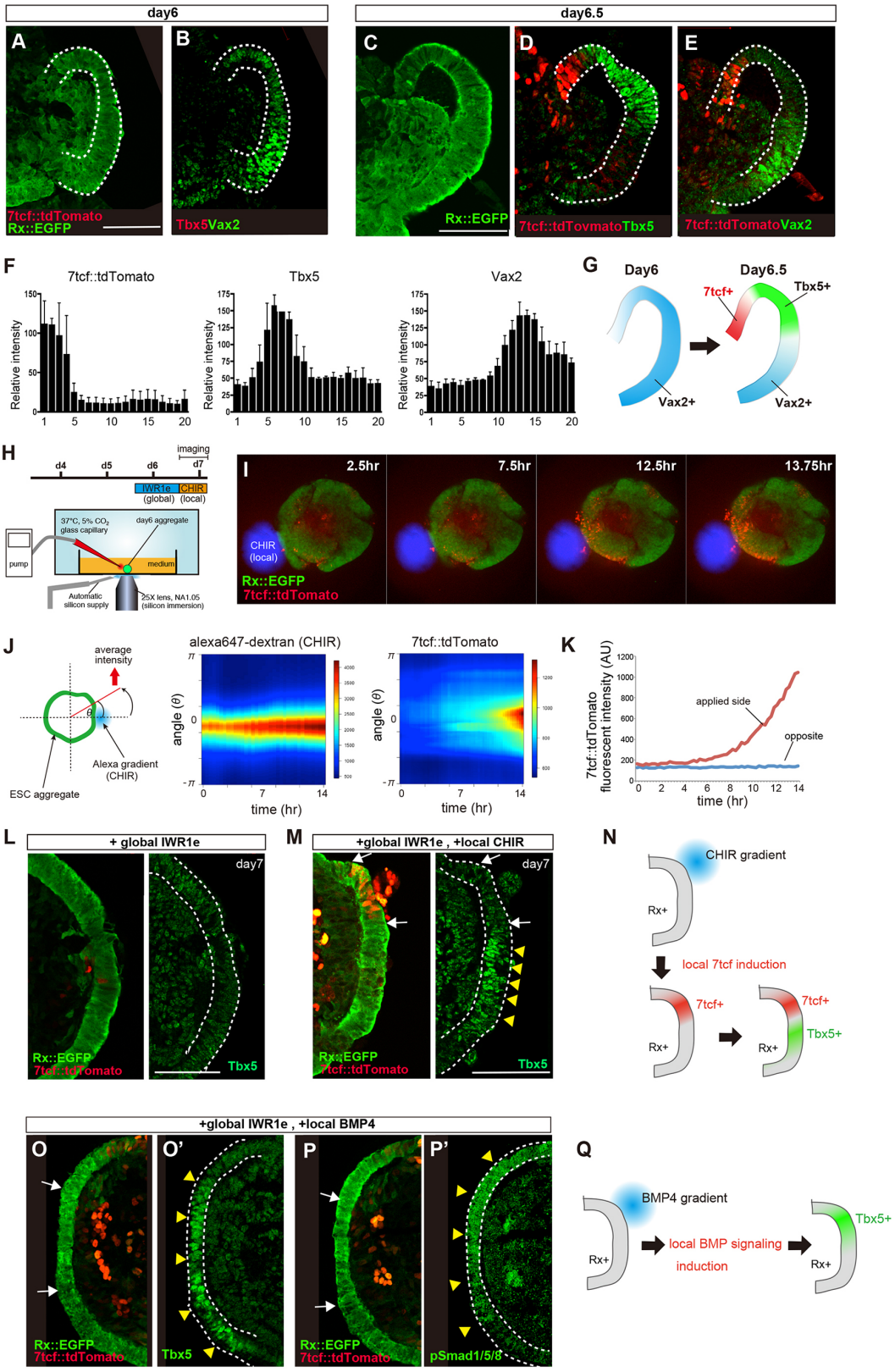

Fig. 5. See next page for legend.

Development (2016) 143, 3895-3906 doi:10.1242/dev.134601

Fig. 5. Local canonical Wnt signaling spatially determined Tbx5 and Vax2 expression in the early mESC-derived optic vesicle-like structure. (A-E) Immunostaining of mESC-derived optic vesicle-like structure using *Rx::EGFP* and *7tcf::H2BtdTomato* cell lines. On day 6, Rx::EGFP (A) and Vax2 (B) expression was detected. On day 6.5, Tbx5 expression was detected adjacent to the Wnt-activated region at the proximal of one side of the optic vesicle (C,D), whereas Vax2 expression was localized on the opposite side of the Wnt-activated region (E). (F) Histograms of relative intensity of 7tcf::H2BtdTomato, Tbx5 and Vax2 expression. The Rx::EGFP$^+$ NR area was divided into 20 parts. From the end of the Wnt-activated side, divided areas were numbered sequentially. Data are mean±s.e.m. of n=3. (G) Schematic of temporal expression of 7tcf::H2BtdTomato, Tbx5 and Vax2 in mESC-derived optic vesicle on day 6-6.5. (H) Schematic of live imaging with local application of drugs. After global treatment of Rx$^+$ aggregates with 0.5 µM IWR1-endo and washing out, CHIR (7 µM) was locally applied from day 6.5. (I) 2.5 h, 7.5 h, 12.5 h and 13.75 h images after start of local application of CHIR. 7tcf::H2BtdTomato expression was seen after 12.5 h. Blue signal was Alexa Fluor 647-dextran (see Movie 5). (J) Circular intensity profile in differentiating ESC aggregate. Schematic of circle scan analysis. After local application, a line connecting the center point of the Alexa Fluor 647-dextran gradient with the center point of the ESC aggregate was set as 0 angle (θ=0). (K) Intensity of Alexa Fluor 647-dextran gradient and 7tcf fluorescent gradient at each angle over time. 7tcf fluorescence intensity on the applied side elevated gradually, and was not changed on the opposite side. (L,M) Immunostaining of locally applied mESC-derived retinal tissue for Tbx5. With only global treatment of IWR1-endo, Tbx5 was not detected (L), and with local CHIR treatment, Tbx5 expression was detected (yellow arrowheads) in the region adjacent to the Wnt-activated region (between white arrows) (M). (N) Schematic of spatially regulated patterning of 7tcf::H2BtdTomato and Tbx5 expression after local application of CHIR. (O,P) After global treatment of IWR1-endo, local BMP4 treatment induced Tbx5 expression (O′) and pSmad expression (P′). White arrows indicate the NR, which was thinner compared with that in adjacent area. Sections in O and P are consecutive (also see whole images in Fig. S5H-N). (Q) Schematic of spatially regulated patterning of Tbx5 expression by local BMP4 induction. White dots line indicate Rx::EGFP$^+$ NR. Scale bars: 100 µm.

variations in the size of optic vesicles and the timing of the formation of optic cup-like structures, may be related to the absence of interactions with surrounding tissues such as surface ectoderm and periocular mesenchyme. In embryonic retina, interactions with these surrounding tissues could be essential for the robust formation of D-V retinal patterning (Fuhrmann et al., 2000).

D-V morphogenesis in ESC-derived optic cup

We show that the mESC-derived optic cup-like structure is non-axisymmetric and has a cleft structure reminiscent of the optic fissure that is transiently observed in the ventral side of the embryonic optic cup. 3D reconstruction of Tbx5 expression in the retinal tissue revealed that the fissure tended to form at the Tbx5-negative region. These observations support the idea that optic fissure formation results from D-V retinal patterning. Live-imaging analysis revealed that fissure formation is achieved by the retinal tissue-intrinsic mechanism in a timely ordered manner. As seen *in vivo*, invagination started at the side opposite the fissure, and fissure formation was coupled with the polarized invagination processes. In vertebrate retinal development, it has been thought that the optic fissure is formed by folding of the ventral retinal epithelium (Heermann et al., 2015); however, there are no reports showing a detailed process of optic fissure formation by live imaging. Furthermore, it has previously been shown that increased cell proliferation and extensive apoptosis in the ventral optic vesicle might accompany optic fissure formation (Ozeki et al., 2000; Trousse et al., 2001; Morcillo et al., 2006), and in a *Bmp7* mutant mouse, fissure formation was not initiated (Morcillo et al., 2006). However, the molecular mechanisms and tissue dynamics for optic fissure formation are not fully elucidated. With its simple culture methods and applicability to live imaging, our mESC culture system could provide a good platform for studying the cellular dynamics and underlying molecular mechanisms involved in optic fissure formation in future studies.

BMP signaling directly regulates D-V polarization and invagination of NR *in vitro*

We demonstrated that expression of *Tbx2*, *Tbx3* and *Tbx5* was upregulated and *Vax2* expression was downregulated by BMP4 treatment in mESC-derived retinal tissue. In contrast, a BMP antagonist influenced *Tbx5* and *Vax2* expression in exactly the reverse manner. In addition, immunohistochemistry revealed that both pSmad signal and Tbx5 expression were upregulated by BMP4 treatment and downregulated by dorsomorphin. These results are consistent with previously reported mechanisms for retinal D-V patterning in which BMP signaling played a pivotal role in determining dorsal identities through *Tbx5* (Koshiba-Takeuchi et al., 2000; Behesti et al., 2006).

Interestingly, BMP signaling was autonomously activated within mESC-derived neuroepithelium. This observation provides a novel view for induction of BMP signaling, which has been reported to be activated through interaction between optic vesicle and surface ectoderm in mouse and chick embryos (Furuta and Hogan, 1998; Trousse et al., 2001; Muller et al., 2007; Behesti et al., 2006; Steinfeld et al., 2013).

Meanwhile, *in vitro* manipulations of Shh signaling levels had only limited effects on *Tbx5* and *Vax2* expression (Fig. S2A-C). Previously, in a study of the optic cup of Smoothened (Smo, a mediator of Shh signaling) conditional knockout mice, *Vax2* expression was found to be downregulated (Zhao et al., 2010). However, in the optic cup of *Gli* (a transcription factor in the Shh pathway) mutant mice, *Vax2* expression was not changed (Furimsky and Wallace, 2006). Further elucidation of the roles of Shh signaling in D-V polarization is required.

One intriguing aspect of the inhibitor assays was that neither the BMP nor the Shh inhibitor substantially suppressed *Vax2* expression (Fig. 3A, Fig. S2A,B). Additionally, we observed that Vax2 expression precedes Tbx5 expression in mESC-derived optic vesicle (Fig. 5A,B). These data suggest that ventral specification is the default direction of NR tissue, and dorsal specification may require an active process by inductive signaling. In support of this, in *Bmpr1a* and *Bmpr1b* mutant mice, *Vax2* expression is increased and *Tbx5* expression is absent (Murali et al., 2005). In conclusion, we have shown that intrinsic BMP signaling is directly responsible for D-V polarization and invagination through regulation of *Tbx5* and *Vax2* in mESC-derived optic cup-like structures.

Canonical Wnt signaling locally activates the BMP signaling pathway

In our qPCR results, inhibition of the canonical Wnt signaling pathway at the early optic vesicle stage (before day 5) and at a later optic vesicle stage (before day 7) gave rise to a marked reduction of *Tbx5* and *Bmp4* expression (Fig. 4C,D), suggesting that canonical Wnt signaling is essential for dorsal induction and maintenance. The necessity of canonical Wnt signaling for maintenance of dorsal identity has already been reported (Veien et al., 2008; Zhou et al., 2008; Hägglund et al., 2013). In this study, we visualized canonical Wnt signaling dynamics. We found that Wnt activity started to spontaneously increase at the proximal portion of one side of the hemispherical vesicle. This pattern is in accord with sequential *Wnt2b* expression *in vivo* (Cho and Cepko, 2006). This biased expression may make a difference in the speed of maturation of RPE between the prospective dorsal and ventral sides to form

Development (2016) 143, 3895-3906 doi:10.1242/dev.134601

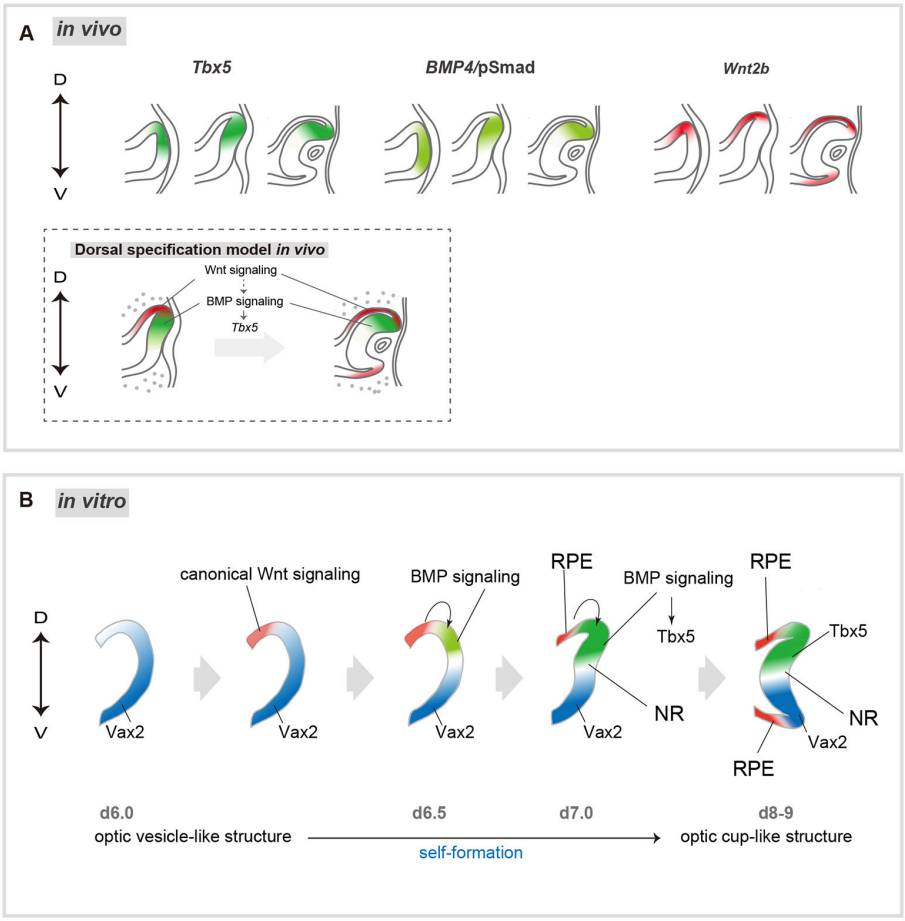

Fig. 6. Model of D-V patterning within mESC-derived retinal neuroepithelium, integrating sequential local BMP and canonical Wnt signaling. (A) Summary of the expression pattern of *Tbx5*, *Bmp4*/pSmad and *Wnt2b* in the developing murine eye based on *in situ* hybridization and immunohistochemistry presented in prior publications (Behesti et al., 2006; Hägglund et al., 2013; Yun et al., 2009; Furuta and Hogan, 1998; Liu et al., 2006). The schema below shows possible dorsal specification model including BMP and Wnt signaling *in vivo*. Gray dots indicate periocular mesenchyme. (B) Model of optic D-V patterning *in vitro* based on the current analysis. In this model, we propose that sequential local BMP and canonical Wnt signaling induce and maintain dorsal identity during morphogenesis. At day 6, Vax2 is expressed within Rx^+ optic vesicle. By day 6.5, canonical Wnt signaling starts at the proximal region of one side. Subsequently, BMP signaling is induced adjacent to the canonical Wnt-activated area, which leads to Tbx5 expression in dorsal NR. From day 7 onwards, cells strongly positive for canonical Wnt mature into RPE with invagination of NR, leading to morphological D-V formation.

morphologic D-V polarity (Fig. 4B). We also found that Vax2 is expressed until day 6 in the optic vesicle. At day 6.5, Tbx5 expression was first detected adjacent to the 7tcf::tdTomato$^+$ area and Vax2 expression was seen in a position opposite (Fig. 5A-G). Additionally, downregulation of *Tbx5* expression by treatment with an inhibitor of the Wnt pathway was rescued by additional BMP4 treatment. These results are consistent with the idea that Vax2$^+$ tissue is a default state of retinal neuroepithelium and the dorsal tissue is induced by specific dorsalizing factors BMPs and Wnts that work upstream of BMP signaling.

When the Wnt agonist CHIR was applied locally to mESC-derived retinal tissue, 7tcf::H2Btdtomato expression appeared in a restricted area. Intriguingly, localized Tbx5 expression was induced by CHIR in the region adjacent to the 7tcf-activated area, which is different to the spatially direct induction by BMP signaling. Because *Tbx5* is downstream of the BMP pathway, these results imply an intrinsic cross-talk between BMP and canonical Wnt signaling, which has been known to exist in several parts of the developing vertebrate embryo (reviewed by Guo and Wang, 2009). For example, in zebrafish dorsal retina, Wnt activity maintains BMP signaling (Veien et al., 2008). The question of how canonical Wnt signaling activated Tbx5 from a flanking portion still remains unclear. A possible explanation is that after the BMP ligand is locally activated by low-level canonical Wnt signaling, BMP expression may be strengthened by autocrine action. Tbx5 expression is induced and augmented in BMP$^+$ cells of Rx$^+$ retina, and then the Tbx5$^+$/BMP$^+$/Rx$^+$ area and Wnt$^+$ area may be regionalized, because in retina, Wnt signaling is repressed by expression of Wnt inhibitor Dickkopf family proteins (DKKs) (Eiraku et al., 2011).

It is also unclear how the Wnt signal is locally activated in the proximal region of the optic vesicle. This may be achieved by the interaction with non-retinal tissues. As we previously described (Eiraku et al., 2011), when the optic vesicle is isolated from the main body of aggregate, the isolated tissue mainly differentiates into neural retina without RPE. This suggests that the non-retinal tissues provide extrinsic cues required for the RPE differentiation at the border between retinal and non-retinal tissue. It has also been demonstrated that Wnt3a treatment promotes RPE differentiation. Based on these previous experiments, BMP signal could be indirectly induced by interaction with non-retinal tissues through local Wnt activation.

Moreover, in our culture system, expression of S-opsin$^+$ photoreceptors in the fully matured retina was shifted with manipulation of the early D-V pattern. Further elucidation of the process for optic D-V regulation may lead to an optimized *in vitro* manipulation of photoreceptor subtypes for future clinical applications.

MATERIALS AND METHODS

Mouse ESC culture

Mouse ESCs (EB5, *Rx::EGFP*, *Rx::EGFP, 7tcf::mCherry* and *Rx::EGFP, 7tcf::tdTomato*) were maintained as previously described (Eiraku et al.,

2011). We define the day on which the SFEBq culture was started as day 0. For axon elongation, on day 12, after adding 10 µg/ml TAG-1 (R&D) on a 0.2 mg/ml poly-D-lysine (Sigma)-coated glass bottom dish (Matsunami) or Petri dish (Falcon), retinal tissue was cultured on 50% collagen gel (Nitta Geratin) in DMEM/F12 medium supplemented with the N2 under 40% O_2/5% CO_2 conditions until day 17. ESC-derived retinal tissues for long-term culture were prepared and maintained as described in supplementary Materials and Methods.

Generation of transgenic/knock-in ESCs

The canonical Wnt signaling reporter line and other transgenic ESCs were prepared as described in supplementary Materials and Methods.

Live imaging

Live imaging analysis was performed as previously described (Eiraku et al., 2011). Briefly, 3D live imaging was performed using specially assembled inverted microscopes (confocal or multi-photon) combined with a full-sized CO_2/O_2 incubator. Optical section images were obtained using a 20× or 25× objective lens (Olympus), a spinning disk confocal system (CSU-X1, Yokogawa) and an EMCCD camera (Andor, 5123512 pixels; the incubation system is based on LCV-110, Olympus). For local application, CHIR or BMP4 was applied with Alexa Fluor 647-conjugated 10000MW dextran (Life Technologies) by pressure ejection from glass pipettes. In Fig. 2J-M, NR apical length was determined by measuring apical surface length of NR. Optic cup depth was defined as the distance between the bottom surface of the optic cup and the line that forms basal turning points in the sectioned image. Fissure depth was measured as the distance between fissure bottom and fissure surface using Imaris software (BitPlane). In Fig. 2J-M, black dots represent measurements of each time point of imaging data demonstrated in Movie 2. The tissue curvature is semi-automatically measured using the widely used three-point method. For preprocessing, the tissue contour was manually extracted from the image. Using our original program, the local curvature is measured as the inverse of radius of the fitting circle. The circle passes three points; one is the sampling point where the curvature is measured, others are at a distance of ±26 mm along the contour from the sampling point. The hinge curvatures are calculated as the maximum values around the dorsal and ventral hinge areas, respectively.

Recombinant proteins and small molecules

Signaling molecules were used as follows: SAG (R&D), cyclopamine-KAAD (Enzo), hBMP4 (R&D), dorsomorphin (Tocris), mWnt3a (R&D), CHIR99021 (Tocris), IWR1-endo (Calbiochem). They were applied to the aggregates in each well on day 5-6.5 or day 7-8.5 prior to the RT-qPCR assay. Total final volume was 150 µl per well and the concentrations of compound are indicated in the text and legends.

Immunohistochemistry

Immunohistochemistry of sectioned samples was performed as described (Eiraku et al., 2011) as detailed in supplementary Materials and Methods. Primary antibodies used for immunohistochemistry are described in Table S1. Antibodies generated in this study were validated by sequential immunohistochemistry in mouse sections, confirming that the immunoreactivities are consisted with the results of *in situ* hybridization previously reported.

In situ hybridization

In situ hybridization was performed based on a previous report (Blackshaw, 2013) as described in supplementary Materials and Methods.

Quantitative PCR

Quantitative PCR was performed using the 7500 Fast Real Time PCR System (Applied Biosystems) using primers described in Table S2. Data were normalized to *Gapdh* expression. The values shown on graphs represent the mean±s.e.m. For inhibitor assay, 24-48 aggregates were examined, and for long-term culture assay 4-12 matured retinal tissues were examined, in duplicate in each experiment, which was repeated at least three times.

Statistical analysis

Statistical tests were performed using PRISM software (GraphPad, v.6). Statistical significance was tested with Student's *t*-test for two-group comparisons and one-way ANOVA with Tukey's post hoc test for multi-group comparison.

Acknowledgements

The authors are grateful to Masatoshi Ohgushi, Yasuhide Furuta, Atsushi Kuwahara and Daiki Nukaya for critical reading and invaluable comments, and to all of the Sasai Lab members for fruitful discussions. This paper is dedicated to Dr Yoshiki Sasai, who passed away suddenly on August 5, 2014.

Competing interests

The authors declare no competing or financial interests.

Author contributions

M.E. and Y.S. designed the research; Y.H., M.K., N.T. and M.E. performed the experiments; Y.H., S.O. and M.E. analyzed the data; Y.H. and M.E. wrote the paper.

Funding

This work was supported by a RIKEN Junior Research Associate Program (Y.H.); Japan Society for the Promotion of Science KAKENHI [24680037 to M.E.]; grants-in-aid from the Ministry of Education, Culture, Sports, Science, and Technology (to Y.S. and M.E.); and the Network Program for Realization of Regenerative Medicine (to Y.S.) from the Japan Science and Technology Agency.

Supplementary information

Supplementary information available online at
http://dev.biologists.org/lookup/doi/10.1242/dev.134601.supplemental

References

Alfano, G., Conte, I., Caramico, T., Avellino, R., Arnò, B., Pizzo, M. T., Tanimoto, N., Beck, S. C., Huber, G., Dollé, P. et al. (2011). Vax2 regulates retinoic acid distribution and cone opsin expression in the vertebrate eye. *Development* **138**, 261-271.

Applebury, M. L., Antoch, M. P., Baxter, L. C., Chun, L. L., Falk, J. D., Farhangfar, F., Kage, K., Krzystolik, M. G., Lyass, L. A. and Robbins, J. T. (2000). The murine cone photoreceptor: a single cone type expresses both S and M opsins with retinal spatial patterning. *Neuron* **27**, 513-523.

Behesti, H., Holt, J. K. L. and Sowden, J. C. (2006). The level of BMP4 signaling is critical for the regulation of distinct T-box gene expression domains and growth along the dorso-ventral axis of the optic cup. *BMC Dev. Biol.* **6**, 62.

Behesti, H., Papaioannou, V. E. and Sowden, J. C. (2009). Loss of Tbx2 delays optic vesicle invagination leading to small optic cups. *Dev. Biol.* **333**, 360-372.

Blackshaw, S. (2013). High-throughput RNA in situ hybridization in mouse retina. *Methods Mol. Biol.* **935**, 215-226.

Cho, S.-H. and Cepko, C. L. (2006). Wnt2b/β-catenin-mediated canonical Wnt signaling determines the peripheral fates of the chick eye. *Development* **133**, 3167-3177.

Eiraku, M., Takata, N., Ishibashi, H., Kawada, M., Sakakura, E., Okuda, S., Sekiguchi, K., Adachi, T. and Sasai, Y. (2011). Self-organizing optic-cup morphogenesis in three-dimensional culture. *Nature* **472**, 51-56.

Esteve, P., Sandonis, A., Ibañez, C., Shimono, A., Guerrero, I. and Bovolenta, P. (2011). Secreted frizzled-related proteins are required for Wnt/β-catenin signalling activation in the vertebrate optic cup. *Development* **138**, 4179-4184.

Fuhrmann, S., Levine, E. M. and Reh, T. A. (2000). Extraocular mesenchyme patterns the optic vesicle during early eye development in the embryonic chick. *Development* **127**, 4599-4609.

Furimsky, M. and Wallace, V. A. (2006). Complementary Gli activity mediates early patterning of the mouse visual system. *Dev. Dyn.* **235**, 594-605.

Furuta, Y. and Hogan, B. L. M. (1998). BMP4 is essential for lens induction in the mouse embryo. *Genes Dev.* **12**, 3764-3775.

Guo, X. and Wang, X.-F. (2009). Signaling cross-talk between TGF-β/BMP and other pathways. *Cell Res.* **19**, 71-88.

Hägglund, A.-C., Berghard, A. and Carlsson, L. (2013). Canonical Wnt/β-catenin signalling is essential for optic cup formation. *PLoS ONE* **8**, e81158.

Heermann, S., Schütz, L., Lemke, S., Krieglstein, K. and Wittbrodt, J. (2015). Eye morphogenesis driven by epithelial flow into the optic cup facilitated by modulation of bone morphogenetic protein. *eLife* **4**, e05216.

Kobayashi, T., Yasuda, K. and Araki, M. (2010). Coordinated regulation of dorsal bone morphogenetic protein 4 and ventral Sonic hedgehog signaling specifies the dorso-ventral polarity in the optic vesicle and governs ocular morphogenesis through fibroblast growth factor 8 upregulation. *Dev. Growth Differ.* **52**, 351-363.

Koshiba-Takeuchi, K., Takeuchi, J. K., Matsumoto, K., Momose, T., Uno, K., Hoepker, V., Ogura, K., Takahashi, N., Nakamura, H., Yasuda, K. et al. (2000). Tbx5 and the retinotectum projection. *Science* **287**, 134-137.

Liu, H., Thurig, S., Mohamed, O., Dufort, D. and Wallace, V. A. (2006). Mapping canonical Wnt signaling in the developing and adult retina. *Invest. Ophthalmol. Vis. Sci.* **47**, 5088-5097.
McLaughlin, T., Hindges, R. and O'Leary, D. D. M. (2003). Regulation of axial patterning of the retina and its topographic mapping in the brain. *Cur. Opin. Neurobiol.* **13**, 57-69.
Morcillo, J., Martínez-Morales, J. R., Trousse, F., Fermin, Y., Sowden, J. C. and Bovolenta, P. (2006). Proper patterning of the optic fissure requires the sequential activity of BMP7 and SHH. *Development* **133**, 3179-3190.
Morse, D. E. and McCann, P. S. (1984). Neuroectoderm of the early embryonic rat eye. *Invest. Ophthalmol. Vis. Sci.* **25**, 899-907.
Mui, G. H., Hindges, R., OLeary, D. D. M., Lemke, G. and Bertuzzi, A. (2002). The homeodomain protein Vax2 patterns the dorsoventral and nasotemporal axes of the eye. *Development* **129**, 797-804.
Muller, F., Rohrer, H. and Vogel-Hopker, A. (2007). Bone morphogenetic proteins specify the retinal pigment epithelium in the chick embryo. *Development* **134**, 3483-3493.
Murali, D., Yoshikawa, S., Corrigan, R. R., Plas, D. J., Crair, M. C., Oliver, G., Lyons, K. M., Mishina, Y. and Furuta, Y. (2005). Distinct developmental programs require different levels of Bmp signaling during mouse retinal development. *Development* **132**, 913-923.
Nakano, T., Ando, S., Takata, N., Kawada, M., Muguruma, K., Sekiguchi, K., Saito, K., Yonemura, S., Eiraku, M. and Sasai, Y. (2012). Self-formation of optic cups and storable stratified neural retina from human ESCs. *Cell Stem Cell* **10**, 771-785.
Ozeki, H., Ogura, Y., Hirabayashi, Y. and Shimada, S. (2000). Apoptosis is associated with formation and persistence of the embryonic fissure. *Curr. Eye Res.* **20**, 367-372.
Peters, M. A. and Cepko, C. L. (2002). The dorsal–ventral axis of the neural retina is divided into multiple domains of restricted gene expression which exhibit features of lineage compartments. *Dev. Biol.* **251**, 59-73.
Satoh, S., Tang, K., Iida, A., Inoue, M., Kodama, T., Tsai, S. Y., Tsai, M.-J., Furuta, Y. and Watanabe, S. (2009). The spatial patterning of mouse cone opsin expression is regulated by bone morphogenetic protein signaling through downstream effector COUP-TF nuclear receptors. *J. Neurosci.* **29**, 12401-12411.
Steinfeld, J., Steinfeld, I., Coronato, N., Hampel, M.-L., Layer, P. G., Araki, M. and Vogel-Höpker, A. (2013). RPE specification in the chick is mediated by surface ectoderm-derived BMP and Wnt signalling. *Development* **140**, 4959-4969.
Takata, N., Sakakura, E. and Sasai, Y. (2016). Activation of Wnt/ß-catenin signaling in ESC promotes rostral forebrain differentiation in vitro. *In Vitro Cell Dev. Biol. Anim.* **52**, 374-382.
Trousse, F., Esteve, P. and Bovolenta, P. (2001). BMP4 mediates apoptotic cell death in the developing chick eye. *J. Neurosci.* **21**, 1292-1301.
Veien, E. S., Rosenthal, J. S., Kruse-Bend, R. C., Chien, C.-B. and Dorsky, R. I. (2008). Canonical Wnt signaling is required for the maintenance of dorsal retinal identity. *Development* **135**, 4101-4111.
Yang, X.-J. (2004). Roles of cell-extrinsic growth factors in vertebrate eye pattern formation and retinogenesis. *Semin. Cell Dev. Biol.* **15**, 91-103.
Yun, S., Saijoh, Y., Hirokawa, K. E., Kopinke, D., Murtaugh, L. C., Monuki, E. S. and Levine, E. M. (2009). Lhx2 links the intrinsic and extrinsic factors that control optic cup formation. *Development* **136**, 3895-3906.
Zhang, X.-M. and Yang, X.-J. (2001). Temporal and spatial effects of sonic hedgehog signaling in chick eye morphogenesis. *Dev. Biol.* **233**, 271-290.
Zhao, L., Saitsu, H., Sun, X., Shiota, K. and Ishibashi, M. (2010). Sonic hedgehog is involved in formation of the ventral optic cup by limiting Bmp4 expression to the dorsal domain. *Mech. Dev.* **127**, 62-72.
Zhou, C.-J., Molotkov, A., Song, L., Li, Y., Pleasure, D. E., Pleasure, S. J. and Wang, Y.-Z. (2008). Ocular coloboma and dorsoventral neuroretinal patterning defects in Lrp6 mutant eyes. *Dev. Dyn.* **237**, 3681-3689.